Supplemental Information for:

Caged naloxone reveals opioid signaling deactivation kinetics

Matthew R. Banghart, John T. Williams, Ruchir C. Shah, Luke D. Lavis, and Bernardo L. Sabatini

Molecular Pharmacology

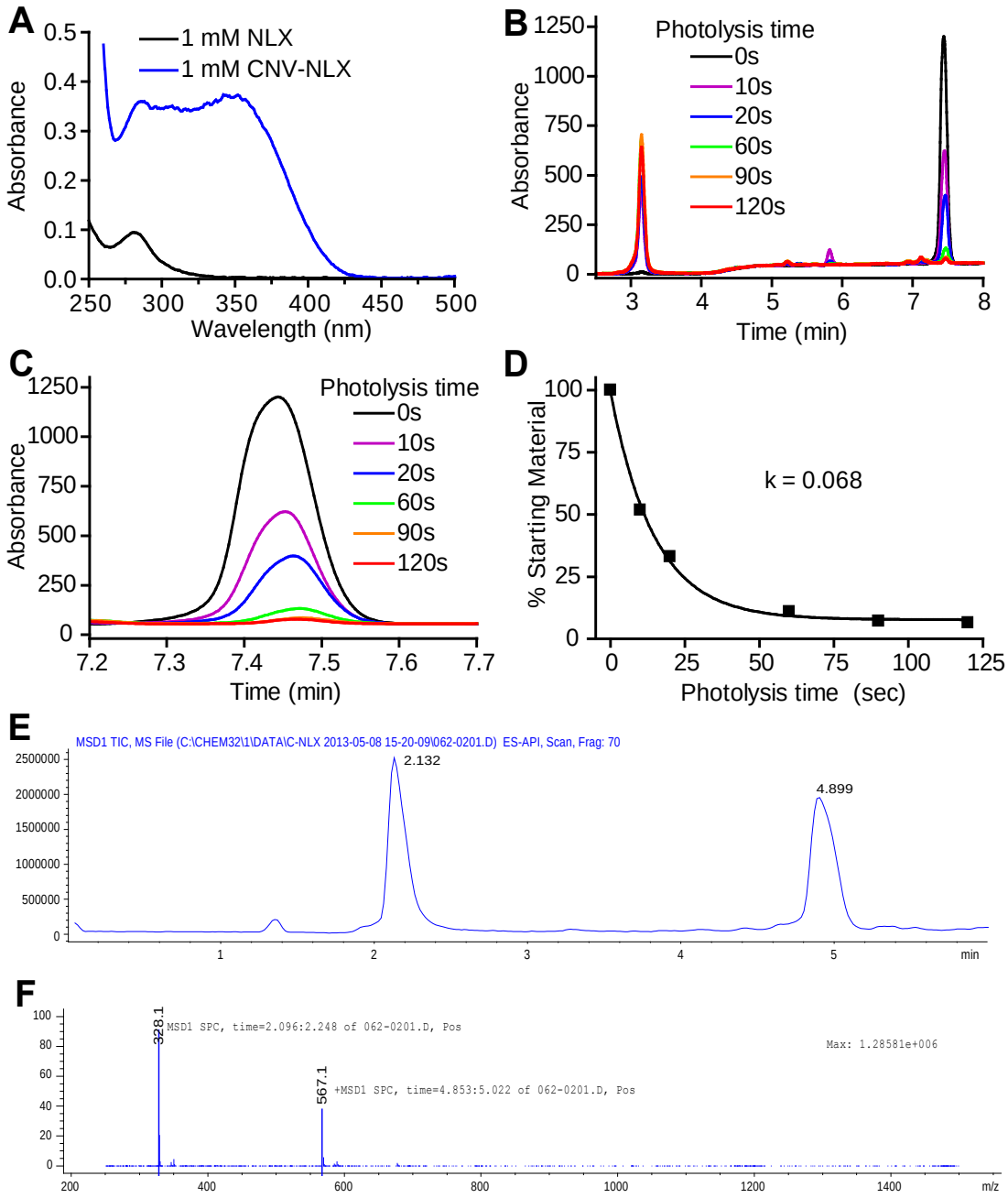

Figure S1. Photolysis of CNV-NLX with blue light. A, UV/VIS absorbance spectra of NLX and CNV-NLX. B, Superimposed HPLC chromatograms of samples of CNV-NLX in phosphate buffered saline that were irradiated for various time periods with 405 nm light. C, Close-up of the CNV-NLX peak from panel B. D, Time course of the uncaging reaction under these conditions determined by the measuring the loss of CNV-NLX over time using the data shown in panels B and C. E, LC-MS total ion current (TIC) chromatogram of a sample of CNV-NLX after an exposure to 405 nm light that led to partial photolysis. D, Mass spectra of the peaks observed in C, which correspond to the protonated cations of NLX (328.1) and CNV-NLX (567.1), respectively.

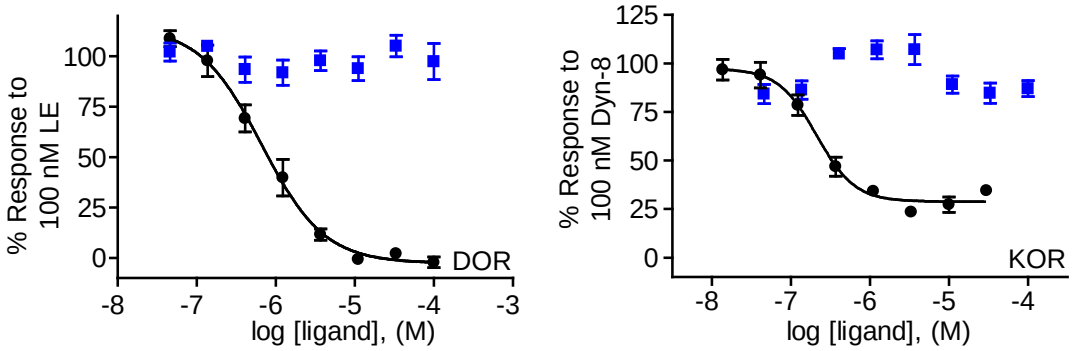

Figure S2. Inactivity of CNV-NLX at delta and kappa opioid receptors. Dose-response curves of NLX (black circles) and CNV-NLX (blue squares) at the delta (*left*) and kappa (*right*) opioid receptors in the presence of 100 nM LE (*n*=6 wells), and 100 nM Dyn-8 (*n*=6 wells) respectively.

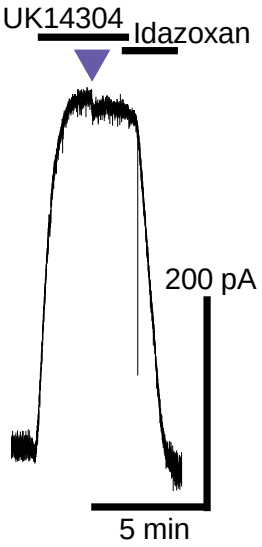

Figure S3. Photolysis of CNV-NLX does not affect currents induced by the α-adrenergic receptor agonist UK14304. Only an artifactual transient inward current is produced by the 405 nm light flash, independent of CNV-NLX photolysis. In the absence of CNV-NLX, the uncaging stimulus still produces a small, transient inward current superimposed on the α-adrenergic receptor-mediated current. Purple triangle indicates a 5 s flash of 405 nm light.

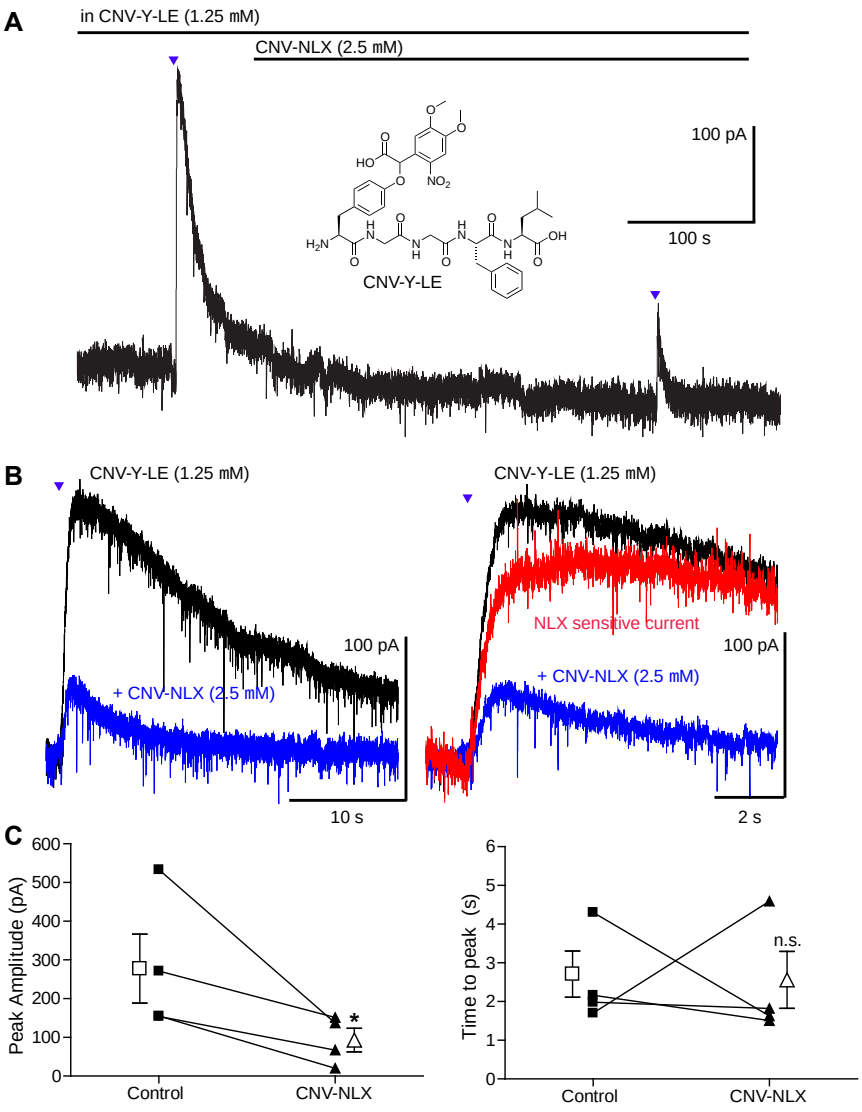

Figure S4: NLX association with MOR occurs with a time constant faster than 1 s. A, Example of a kinetic competition experiment with caged agonist (CNV-Y-LE) and CNV-NLX, which are both caged by a CNV group on their phenol and thus have near identical photochemical properties. The chemical structure of CNV-Y-LE is shown as well. B, (left) Zoom-in of the superimposed currents obtained in the absence (black) and presence (blue) of CNV-NLX, and (right) further zoom of the rising phase with the NLX sensitive current obtained by subtracting the blue from the black trace, shown in red. Photolysis of caged agonist alone activates a large outward current with a time constant of 279±19 ms. C, Summary plots (n=4 cells) showing that including CNV-NLX reduces the peak current evoked by agonist uncaging (left) without affecting the kinetics of activation (right). Asterisks denote a significant difference from the "no flash" condition ($p < 0.05$) according to paired sample t-test analysis. These data indicate that NLX associates with MORs faster than LE activates GIRKs via MORs. Therefore, NLX association occurs too quickly to contribute to the tau decays measured in this study.

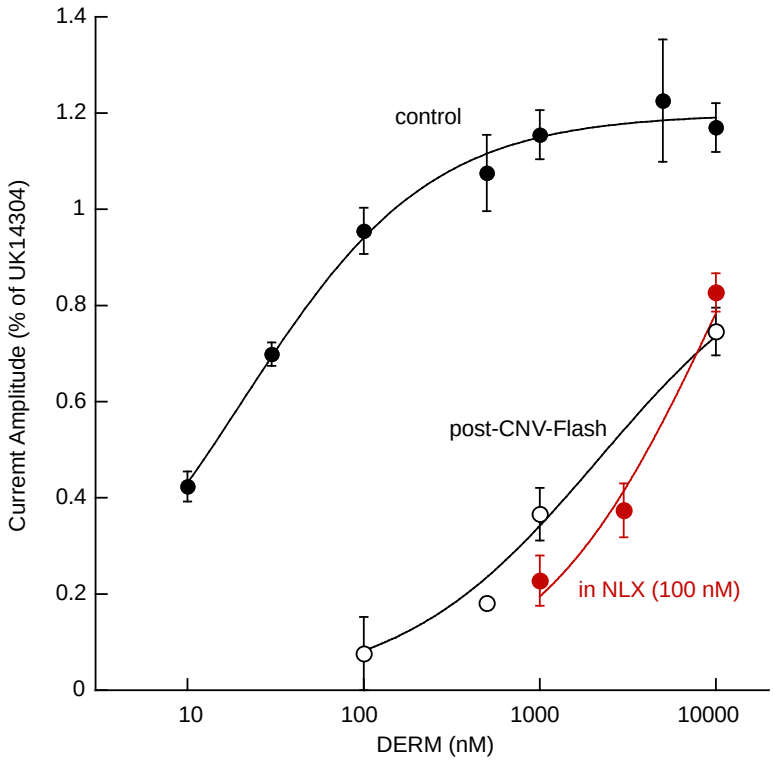

Figure S5: A 5s flash of 405 nm light releases approximately 100 nM NLX. Amplitude-normalized dose response curves of DERM in the presence of 5 μM CNV-NLX before (filled black circles) and after photolysis (empty black circles), or of DERM in the presence of 100 nM NLX after pre-treatment with antagonist (red circles). The post-flash DERM currents approximately match the currents evoked in the presence of 100 nM NLX. Therefore at least 100 nM NLX is released by the light flash, although this could be an underestimate because the photolysis measurements are not at steady state.

Table S1 discussion

At least two distinct agonist affinity states have been identified that are dependent on the coupling of G-proteins to GPCRs (Childers and Snyder, 1980). Initial binding occurs through a high affinity state but after GDP-GTP exchange, the GTP-bound activated state from which the agonists dissociate in our study has been shown to exhibit lower affinity for agonists. Most competition radioligand binding studies report binding constants (as K_i) for the high affinity state, (Raynor et al., 1994; Raynor et al., 1995) and low-affinity state binding constants are available under a single condition for only 7 of the 11 compounds used in our study (McPherson et al., 2010). To most accurately represent the low-affinity state when comparing deactivation-rates, we adjusted the high affinity values for the remaining 4 agonists by comparing the two studies (Table S1). For the 5 compounds reported under both conditions, we calculated a 1.25 ± 0.11 fold difference in pKi between the high and low affinity states. Scaling the available high-affinity binding constants by this factor yielded a complete list of low-affinity binding constants (Final pK_i) for comparison to deactivation rate.

Agonist	High pK_i	Low pK_i	pK_i ratio	Calc'd Low pK_i	Final pK_i	Mean Tau decay (s) ± SEM (N)
β-endorphin	9.00			7.21	7.21	10.80 ± 1.24 (8)
etorphine	9.64	8.46	1.14	7.72	8.46	9.35 ± 1.64 (5)
endomorphin-1		6.55			6.55	3.68 ± 0.20 (5)
dermorphin	9.48			7.59	7.59	3.37 ± 0.28 (5)
methadone	7.72	6.26	1.23	6.18	6.26	2.41 ± 0.20 (7)
morphine	7.66	6.60	1.16	6.13	6.60	1.77 ± 0.22 (8)
oxycodone		5.81			5.81	1.64 ± 0.12 (5)
DSLET	7.41			5.93	5.93	1.51 ± 0.20 (6)
ME	9.19	6.55	1.40	7.35	6.55	1.36 ± 0.07 (8)
DAMGO	8.70	6.64	1.31	6.96	6.64	1.22 ± 0.14 (5)
codeine	6.77			5.42	5.42	1.12 ± 0.29 (4)

Table S1. Conversion of high-affinity to low-affinity binding constants for comparison to deactivation rates. Competition radioligand binding constants obtained under conditions favoring the high-affinity state, the low-affinity state, the ratio of high/low, the calculated low-affinity binding constant for agonists for which only high-affinity binding constants are available, the final list of binding constants used for analysis, and the corresponding deactivation rates measured in this study. All of the competition radioligand binding assays were performed on isolated membranes from cells expressing rat MOR.

References

Childers, S. R., Snyder, S. H. (1980) Differential regulation by guanine nucleotides or opiate agonist and antagonist receptor interactions. *J Neurochem* **34**: 583-93.

McPherson, J., Rivero, G., Baptist, M., Llorente, J., Al-Sabah, S., Krasel, C., Dewey, W. L., Bailey, C. P., Rosethorne, E. M., Charlton, S. J., Henderson, G., Kelly, E. (2010) mu-opioid receptors: correlation of agonist efficacy for signalling with ability to activate internalization. *Mol Pharmacol* **78**: 756-66.

Raynor, K., Kong, H., Chen, Y., Yasuda, K., Yu, L., Bell, G. I., Reisine, T. (1994) Pharmacological characterization of the cloned kappa-, delta-, and mu-opioid receptors. *Mol Pharmacol* **45**: 330-4.

Raynor, K., Kong, H., Mestek, A., Bye, L. S., Tian, M., Liu, J., Yu, L., Reisine, T. (1995) Characterization of the cloned human mu opioid receptor. *J Pharmacol Exp Ther* **272**: 423-8.